

# Tracking of the dynamic localization of the Rab-specific HOPS subunits reveal their distinct interaction with Ypt7 and vacuoles

Kathrin Auffarth, Henning Arlt, Jens Lachmann, Margarita Cabrera and Christian Ungermann\*

Biochemistry section; Department of Biology/Chemistry; University of Osnabrück; Osnabrück, Germany

**Keywords:** HOPS, tethering complex, Vps39, Vps41, endosome, vacuole

Endosomal and vacuole fusion depends on the two homologous tethering complexes CORVET and HOPS. HOPS binds the activated Rab GTPase Ypt7 via two distinct subunits, Vps39 and Vps41. To understand the participation and possible polarity of Vps41 and Vps39 during tethering, we used an *in vivo* approach. For this, we established the ligand-induced relocalization to the plasma membrane, using the Mon1-Ccz1 GEF complex that activates Ypt7 on endosomes. We then employed slight overexpression to compare the mobility of the HOPS-specific Vps41 and Vps39 subunits during this process. Our data indicate an asymmetry in the Rab-specific interaction of the two HOPS subunits: Vps39 is more tightly bound to the vacuole, and relocates the entire vacuole to the plasma membrane, whereas Vps41 behaved like the more mobile subunit. This is due to their specific Rab binding, as the mobility of both subunits was similar in *ypt7Δ* cells. In contrast, both HOPS subunits were far less mobile if tagged endogenously, suggesting that the entire HOPS complex is tightly bound to the vacuole *in vivo*. Similar results were obtained for the endosomal association of CORVET, when we followed its Rab-specific subunit Vps8. Our data provide *in vivo* evidence for distinct Rab specificity within HOPS, which may explain its function during tethering, and indicate that these tethering complexes are less mobile within the cell than previously anticipated.

## Introduction

Protein transport via the endosome toward the lysosome depends on multiple fission and fusion events. Endocytic vesicles fuse with the early endosome, which then undergoes multiple membrane remodeling, fission and fusion processes to generate intraluminal vesicles and allow for the recycling of receptors.<sup>1</sup> As a consequence, late endosomes are formed, which finally fuse with the lysosome/vacuole.<sup>2</sup>

Fusion of membranes follows a coordinated order of membrane recognition and tethering and subsequent bilayer mixing. Among the many diverse factors implicated in fusion along the endomembrane system, Rab GTPases, tethering factors and SNAREs seem to be the conserved machinery that is found in all cases.<sup>3,4</sup> Rabs function as molecular switches, which require a guanine nucleotide exchange factor (GEF) for their activation to the GTP-form. They can then interact with effectors such as tethering factors or lipid kinases, and are turned over to the GDP-form after interaction with their specific GTPase activating protein (GAP).<sup>5,6</sup> Within the endocytic pathway, Rab5 resides on early endosomes and is replaced by Rab7 on late endosomes.<sup>2,7</sup> Activation of Rab5 occurs via Vps9-domain containing proteins such as Rabex-5,<sup>8,9</sup> whereas the Mon1-Ccz1 complex generates Rab7-GTP.<sup>10,11</sup>

Two homologous heterohexameric tethering complexes have been identified as specific effectors of both Rabs. The CORVET complex binds to the Rab5-like Vps21, whereas the HOPS complex is an effector of activated Rab7/Ypt7 in yeast.<sup>12-16</sup> Both complexes share four central subunits, Vps11, 16, 18 and the SNARE-binding Vps33 subunit. The recent overall structure of the HOPS complex showed that the two Rab-specific subunits Vps41 and Vps39 reside at opposite ends of a seahorse-like particle of some 30 nm.<sup>3</sup> In analogy, it is likely that the Vps41-homolog Vps8 and the Vps39-like Vps3 subunit are positioned similarly in CORVET. Indeed, both complexes can tether Vps21 and Ypt7-decorated membranes *in vitro*.<sup>17-19</sup>

It is surprising that both tethering complexes use two different subunits to interact with the same Rab GTPase.<sup>3,19,20</sup> Within HOPS, Vps41 is known to also bind the AP-3  $\delta$ -subunit Apl5,<sup>21,22</sup> presumably as a prerequisite of fusion of AP-3 vesicles with vacuoles.<sup>23,24</sup> For Vps39, additional binding partners outside HOPS beyond Ypt7 have not been identified. To begin to understand the asymmetry within HOPS, we decided to follow the dynamic localization of Vps41 and Vps39 within cells by employing an adapted protocol of a rapamycin-induced heterodimerization.<sup>25,26</sup> Our data reveal that Vps39 interacts more closely with vacuoles than the more mobile subunit Vps41. However, if both subunits

\*Correspondence to: Christian Ungermann; Email: cu@uos.de

Submitted: 03/03/14; Revised: 04/29/14; Accepted: 05/09/14; Published Online: 05/12/14

Citation: Auffarth K, Arlt H, Lachmann J, Cabrera M, Ungermann C. Tracking of the dynamic localization of the Rab-specific HOPS subunits reveal their distinct interaction with Ypt7 and vacuoles. Cellular Logistics 2014; 4:e29191; <http://dx.doi.org/10.4161/cl.29191>

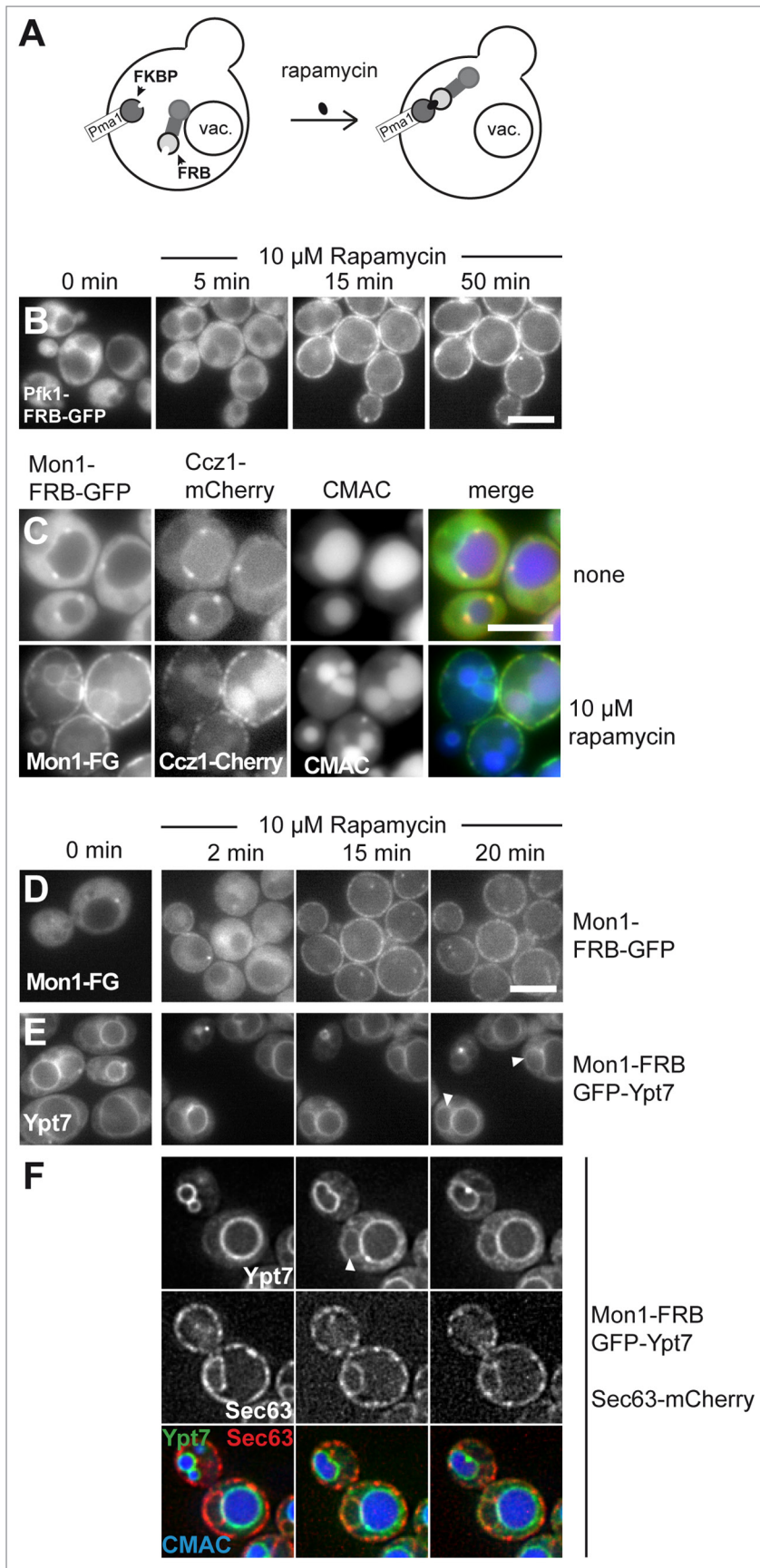


**Figure 1.** Monitoring of dynamic relocalization of the endosomal GEF complex. **(A)** Model of rapamycin induced relocalization of tagged proteins to the plasma membrane. **(B)** Establishment of the rapamycin-induced relocalization. Pfk1 was C-terminally tagged with FRB-GFP in a strain expressing Pma1-FKBP. Cells were monitored without rapamycin (0 min). Then 10  $\mu$ M rapamycin was added, and cells embedded in agar were monitored for 50 min at 26  $^{\circ}$ C by fluorescence microscopy. Three time-points are shown. **(C)** The endosomal GEF complex relocalizes together to the plasma membrane. Mon1-FRB-GFP was expressed from the *TEF1* promoter in cells expressing Ccz1-mCherry. Cells were stained with CMAC to label the vacuole and analyzed in the absence and presence of 10  $\mu$ M rapamycin. Top, cells without rapamycin, bottom, cells after overnight incubation with rapamycin. **(D)** Time-course of Mon1-relocalization. Mon1-FRB-GFP under the control of the *TEF1* promoter was observed in the absence and presence of 10  $\mu$ M rapamycin at the indicated time points. **(E-F)** Localization of Ypt7 upon relocalization of Mon1 to the plasma membrane. Mon1-FRB was co-expressed with GFP-tagged Ypt7, and Ypt7 was analyzed by fluorescence microscopy. Analysis was as in **(D)**. White arrows indicate nuclear ER localization of Ypt7. In **(F)**, the same strain also contained Sec63-mCherry to monitor the ER. Cells were stained with CMAC to observe the vacuole, and analyzed in the presence of 10  $\mu$ M rapamycin.

are integrated into the HOPS complex, the entire complex is found primarily on vacuoles and is less mobile. Our data suggest that HOPS is primarily localized to vacuoles via Vps39, where it interacts with incoming membranes.

## Results

Recent studies used the ligand-induced heterodimerization as an approach to achieve acute inactivation or relocalization of proteins.<sup>25-28</sup> We decided to establish this method to follow the dynamics of Rab interacting proteins at endosome and vacuole.

For the relocalization assay we used a rapamycin-insensitive yeast strain, which expressed a FK506 binding protein of 12 kD (FKBP12) fused to the plasma membrane ATPase Pma1.<sup>25</sup> Pma1 is rather abundant<sup>29</sup> and localizes in distinct domains at the plasma membrane.<sup>30</sup> Thus, proteins tagged with the small FKBP12-rapamycin binding domain of the human Tor1 (FRB) should localize to the plasma membrane upon addition of rapamycin (Fig. 1A). As a first test, we fused a dual FRB-GFP tag to the abundant cytosolic phosphofructokinase 1 (Pfk1) and monitored cells over time (Fig. 1B). To be able to correlate the appearance of Pfk1 at the plasma

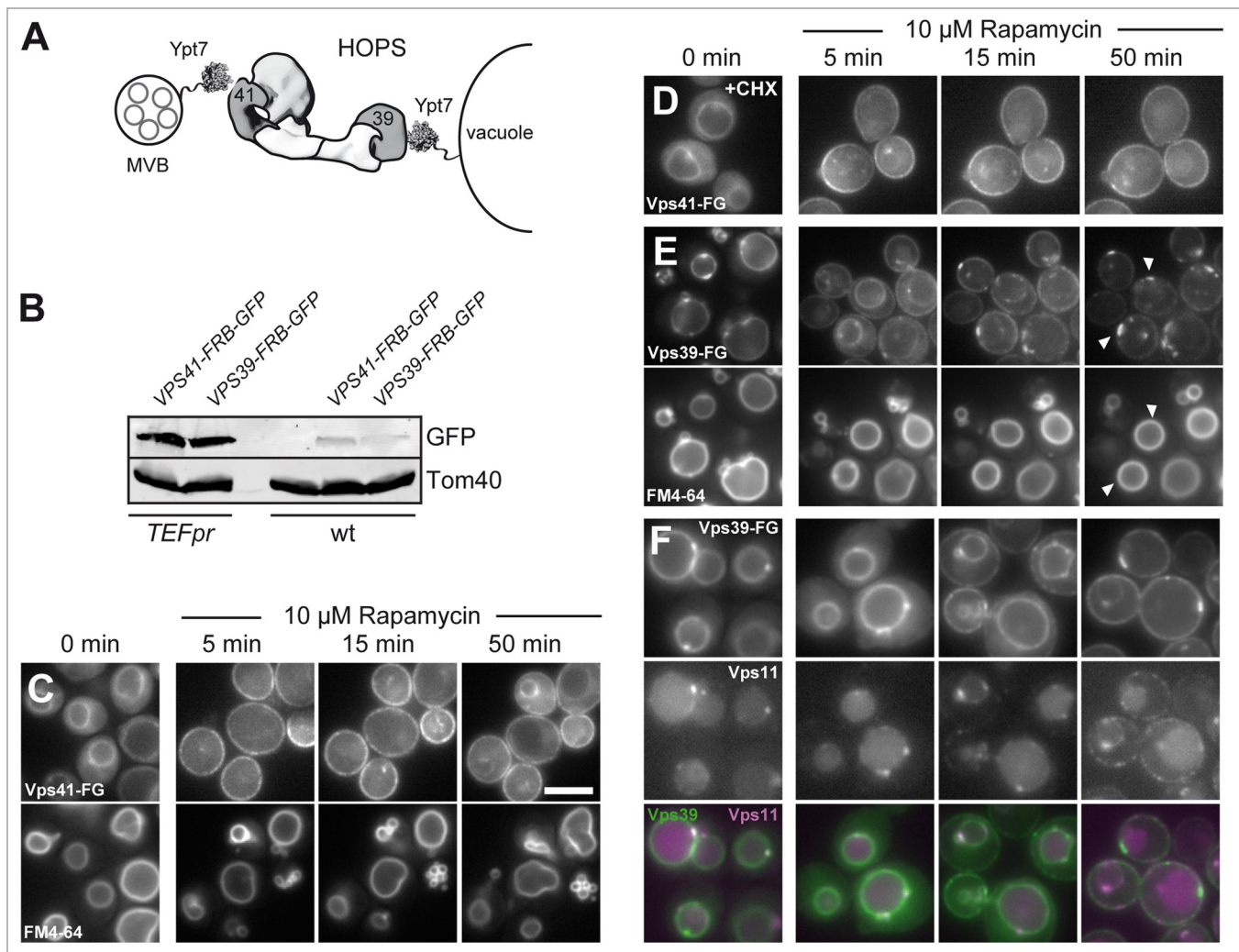


**Figure 2.** Dynamic relocation of the HOPS-specific Vps39 and Vps41. **(A)** Model of HOPS function between membranes. Ypt7 is present on multi-vesicular bodies (MVBs) and vacuoles and binds to HOPS via Vps41 and Vps39. HOPS is shown as a structural model based on the electron microscopy structure.<sup>3</sup> **(B)** Expression levels of Vps41 and Vps39 in wild-type and overexpression condition was analyzed by loading similar amounts of cell lysate onto SDS-PAGE gels. Proteins were detected after western blotting using anti-GFP to detect Vps41 and Vps39, and anti-Tom40 antibody as loading control. **(C-E)** Dynamic relocation of the two Rab-specific HOPS subunits Vps41 and Vps39. The indicated subunits were placed under the control of the *TEF1* promoter and tagged with FRB-GFP and analyzed as in Figure 1. In **(C)**, FM4-64 staining was done in Vps41-FRB-GFP expressing cells to analyze vacuole morphology during the time course. In **(D)**, 10  $\mu$ M of the translation inhibitor cyclohexamide was added before rapamycin addition. The same result was obtained with 50  $\mu$ M cyclohexamide (not shown). **(E)** Vps39-FRB-GFP was analyzed, and vacuolar contacts to the plasma membrane are indicated by arrows. The bottom panel shows vacuolar straining as in **(C)**. In **(F)**, Vps11 was tagged with mCherry in the strain carrying Vps39-FRB-GFP, and analysis was done as in **(E)**. Size bar is 5  $\mu$ m.

membrane with the loss of the cytosolic signal, we followed immobilized cells on a heated slide over time. Pfk1-FRB-GFP was initially entirely cytosolic, but shifted to the plasma membrane upon addition of 10  $\mu$ M rapamycin. We observed a clear signal in the cell periphery already after 15 min, which increased further in the next 50 min and led to a depletion of the cytosolic GFP-signal (Fig. 1B).

#### Dynamic relocation of Mon1-Ccz1 affects Ypt7 activation

We then used this assay to analyze the dynamics of Rab-specific complexes at endosomes and vacuole. We focused on the Mon1-Ccz1 GEF complex, which activates Ypt7 at the late endosome and vacuole.<sup>10</sup> Mon1, fused to the dual FRB-GFP tag,

was initially localized to endosomal dots proximal to the vacuole, which colocalized with mCherry-tagged Ccz1 (Fig. 1C, top). Upon overnight incubation in 10  $\mu$ M rapamycin, both proteins relocated to the plasma membrane and resulted in partial vacuole fragmentation after this long time period (Fig. 1C). Loss of endosomal localization could be observed already at 2 min after rapamycin addition, indicating that Mon1-Ccz1 is dynamically associated with the endosome (Fig. 1D), and that a peripheral membrane protein complex of the endocytic pathway can be relocated via the ligand-induced heterodimerization.

To obtain insights into the functional consequences of Mon1-Ccz1 relocation, we followed GFP-tagged Ypt7 in strains expressing Mon1-FRB. Upon rapamycin addition, Ypt7 partially

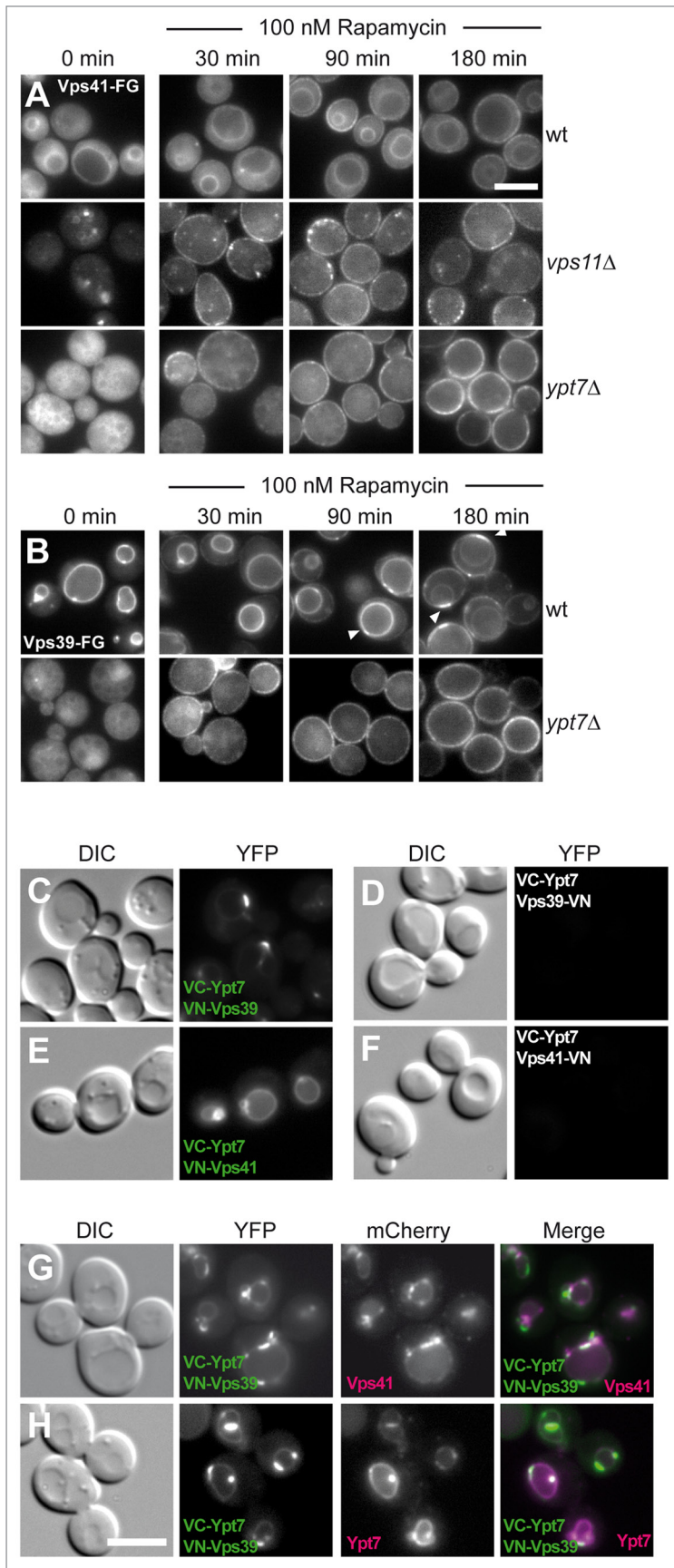


**Figure 3.** Vps41 and Vps39 differ in vacuole affinity and colocalization with Ypt7. (A, B) Vps41 and Vps39 relocalize more efficiently in the absence of Ypt7. FRB-GFP tagged Vps41 (A) and Vps39 (B) were observed as in Figure 2 by fluorescence microscopy in the indicated strains. To resolve their dynamic relocalization over time, 100 nM rapamycin was added to the cells. (C-H) Vps41 and Vps39 differ in their Ypt7-interaction on vacuoles as revealed by the Split-YFP approach. Ypt7 was tagged with the C-terminal half of Venus (VC) in all strains, whereas Vps39 and Vps41 were tagged N-terminally (C, E) or C-terminally (D, F) with the VN part.<sup>34</sup> For colocalization analysis, the cells expressing VC-Ypt7 and VN-Vps39 were additionally modified by tagging Vps41 with mCherry (G) or transformed with a CEN plasmid expressing dsRED-Ypt7 under the control of a *PHO5* promoter (H). All cells were observed by fluorescence microscopy. Scale bar, 5 μM.

shifted to the nuclear ER (Fig. 1E, white arrows), confirmed by colocalization with the ER-residing marker Sec63 (Fig. 1F). Indeed, we recently showed that inactivation of GEFs results in the relocalization of Rabs to the ER.<sup>31</sup> Thus, we demonstrate that the relocalized Mon1-Ccz1 was not sufficient to recruit the Rab7 homolog Ypt7 to the plasma membrane, suggesting the need of additional or other recruitment factors for the Rab GTPase in yeast. As a consequence, downstream processes, as the efficient activation of Ypt7, are disturbed.

#### The HOPS-specific Vps39 and Vps41 show differences in their localization behavior

Having established the basic conditions for relocalization of the endosomal GEF complex, we turned to HOPS as a Ypt7 effector complex. As learned from Mon1-Ccz1, we expected that we could follow the dynamics of HOPS subunits, though would not expect defects in vacuole morphology during the periods of our observation. HOPS and its sibling CORVET differ only in their Rab-specific subunits, which in the case of HOPS may support the correct orientation between membranes, with Vps39 being positioned on the vacuole and Vps41 available for incoming cargo from the multivesicular body (MVB) (Fig. 2A).<sup>3,20</sup> Each tethering complex requires the Rab for its membrane localization.<sup>3,32</sup> We thus wondered if we could get further insights on the subunit level by tracing the redistribution of the Rab-specific HOPS subunits Vps41 and Vps39 in our *in vivo* assay.

To monitor the distribution of both Vps41 and Vps39 over a longer period of time in the same cells, we increased the expression levels of the FRB-GFP-tagged subunit using the *TEF* promoter. This resulted in 8–10-fold overexpression of the respective subunit compared with wild-type levels (Fig. 2B). Furthermore, we verified that tagging and overexpression of these subunits had no effect on protein functionality using a CPY sorting assay (not shown).

Under overexpression conditions, Vps41-FRB-GFP was initially found in the cytosol and on the vacuolar rim, but rapidly translocated to the plasma membrane within 5 min, leading to a significant loss of the vacuolar signal

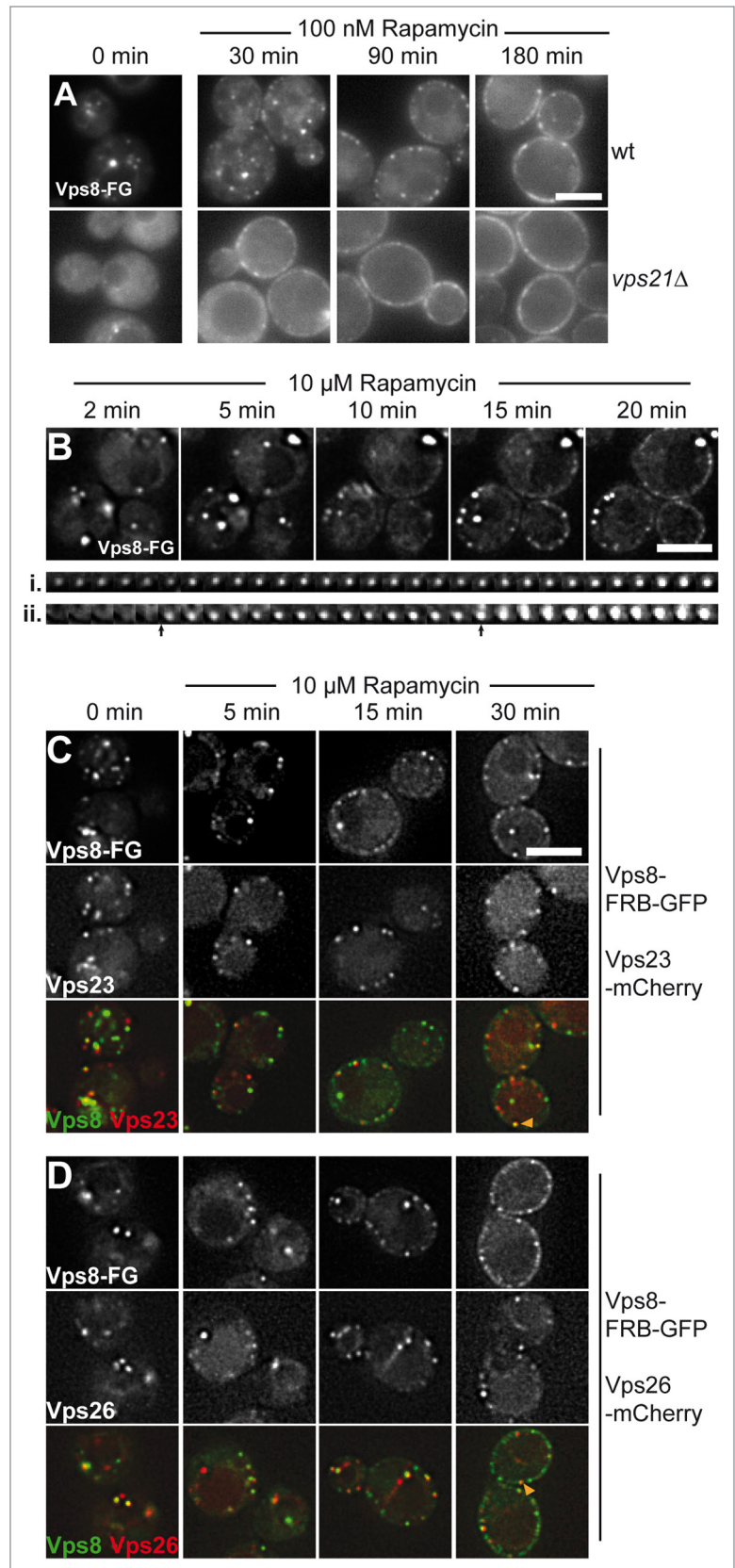
**Figure 4.** CORVET Vps8 relocates with endosomes to the plasma membrane. (A) Vps8 was placed under the control of the *TEF1* promoter and tagged with FRB-GFP. The protein was then monitored in the absence (0 min) and presence of 100 nM rapamycin in wt (top) or *vps21Δ* strains (bottom). (B) Time-resolved dynamics of Vps8 at the plasma membrane. Vps8 was analyzed as in (A) in the presence of 10 μM rapamycin. The bottom trace shows two individual Vps8 positive dots at the plasma membrane position over 20 min with 1 min intervals. Arrows indicate strong changes in fluorescence in the second (ii) trace. (C,D) Entire endosomes relocate with Vps8. Vps23 (B) or Vps26 (C) were C-terminally tagged with mCherry in strains expressing Vps8-FRB-GFP, which was under control of the *TEF1* promoter. Both channels were monitored simultaneously in the absence and presence of rapamycin. Size bars are 5 μm.

(Fig. 2C). Despite this almost complete relocation, the vacuoles showed only a mild fragmentation during this period (Fig. 2C, bottom). To exclude that we would only observe newly synthesized Vps41 in our assay, we added cyclohexamide together with rapamycin to inhibit protein synthesis. However, we observed the similar signal distribution for Vps41 (Fig. 2D). Our data thus indicate that a large portion of Vps41 can be relocated to the plasma membrane without affecting vacuole morphology.

We then turned to the other Ypt7-specific HOPS subunit Vps39. This protein was initially present on vacuoles with almost no cytosolic background (Fig. 2E). Upon rapamycin addition, Vps39 also accumulated at the plasma membrane after 5 min, though unlike Vps41, we still observed a strong vacuolar signal at this time (Fig. 2C vs. E). At later time points, we noticed that a fraction of Vps39 strongly accumulated in patches at the plasma membrane, which coincided with vacuoles (Fig. 2E). When the shared HOPS and CORVET subunit Vps11, tagged with mCherry, was followed in the same strain, it was also present at the plasma membrane, indicating that the Vps39-positive structures also correspond to HOPS (Fig. 2F). These data show that most FRB-tagged Vps39 can be mobilized to the plasma membrane, of which some fraction remains tightly associated with the vacuole surface. We noticed that Vps41 is about 1.5 times more abundant than Vps39 when overexpressed (Fig. 2B), though consider it unlikely that this explains the different behavior of the two proteins.

#### The two Ypt7-interacting HOPS subunits differ in their vacuole affinity

As both Vps41 and Vps39 interact with Ypt7, we asked if their intracellular mobility would behave more similar in the absence of Ypt7. To improve the resolution of the translocation events, we lowered the rapamycin concentration 100-fold and extended the time-course of our observation. In wild-type cells, Vps41 and Vps39 now required more than 90 min to accumulate at the plasma membrane, and efficient accumulation was only



seen at 180 min (Fig. 3A and B). For Vps39, the same patch-like apposition of the vacuole was observed as before. In contrast, in the absence of Ypt7, both Vps39 and Vps41 moved rapidly from

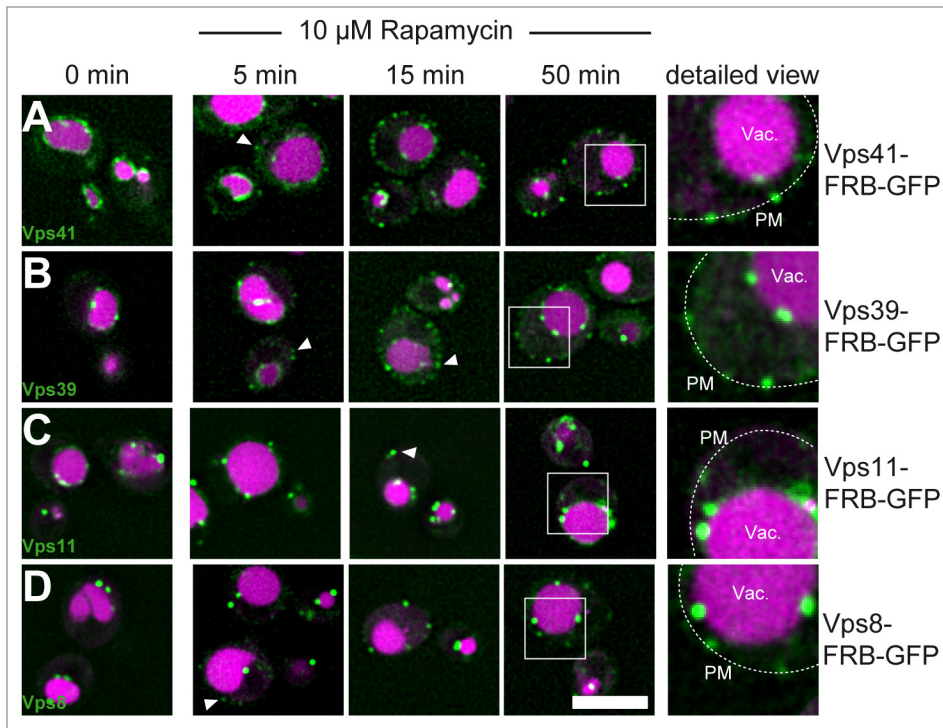


**Figure 5.** Endogenous HOPS is less mobile than its single subunits. (A-C) The indicated HOPS subunits were tagged C-terminally with FRB-GFP and monitored in the presence of 10  $\mu$ M rapamycin at the indicated time points. A detailed view is shown to the right. (D) Endogenous Vps8, tagged with FRB-GFP was observed in the presence of rapamycin as in A. Size bar is 5  $\mu$ m.

their cytosolic distribution to the plasma membrane (Fig. 3A and B). In addition, Vps39 did no longer localize in patches, pointing to an organizational cross-talk between the HOPS subunit and Ypt7. A similar rapid translocation was observed for Vps41, when the HOPS complex integrity was lost in *vps11 $\Delta$*  cells (Fig. 3A).<sup>33</sup> Our data indicate that Ypt7 restricts the intracellular mobility of Vps41 and Vps39 and sequesters Vps39 more tightly to the vacuole surface.

We then asked if we could find further support for the distinct interaction of Vps41 and Vps39 with Ypt7. We therefore turned to the bimolecular fluorescence complementation analysis, where each putative interacting protein was tagged with the N-terminal (VN) or C-terminal (VC) half of the Venus-variant of GFP.<sup>34</sup> Only if interaction of the two proteins is observed, a signal in the YFP channel is observed. Due to the tagging cassette, the detected proteins were also overproduced. We considered this an advantage as we could then distinguish the behavior of both subunits relative to each other.

We indeed detected a strong signal for VC-Ypt7 and VN-Vps39 (Fig. 3C) or VN-Vps41 (Fig. 3E). C-terminal tagging of either protein did not result in any specific signal (Fig. 3D and F), suggesting that the Ypt7-binding site is more proximal to the N-terminal segment of the Rab-specific subunits. Even though both signals were detected on the vacuole, the Ypt7-Vps39 signal was strongly enriched in patches, whereas the Ypt7-Vps41 signal was more uniformly distributed along the vacuolar surface. To analyze the distribution of Vps39 in this context in more detail,

we also tagged Vps41 (Fig. 3G) and Ypt7 (Fig. 3H) in the same strain with mCherry. Whereas Ypt7 completely colocalized with the YFP signal (Fig. 3H), some Ypt7-Vps39 signal was also observed in separate patches from Vps41. In combination, these data provide further support that Vps39 and Vps41 behave different from each other also along the vacuolar surface and that a pool of Ypt7-Vps39 exists independently of Vps41.

#### CORVET Vps8 interacts strongly with its target membrane

We next wondered if this apparent polarity within HOPS could be extended to CORVET. As endosomes are rather small, such a comparison did not seem feasible. In addition, Vps3 accumulated strongly in the cytosol upon overproduction,<sup>35</sup> thus leaving us with Vps8 to monitor at least the mobility of CORVET. We tagged Vps8 as before and followed its dot-like localization, which reflect clustered multivesicular bodies, a result of the Vps8 overexpression<sup>35</sup>(Fig. 4A).

When rapamycin was added in a low concentration, Vps8 dots disappeared at the expense of several puncta at the plasma membrane over the course of the experiment. Similar to our observations on HOPS, the redistribution of Vps8 was strongly enhanced in the absence of the interacting Rab GTPase Vps21 (Fig. 4A). When we used a higher rapamycin concentration to reallocate Vps8 faster, we could follow Vps8 in the same cells over a period of 20 min (Fig. 4B). When we traced single Vps8-positive dots at the plasma membrane over time, we noticed two different populations with gradual (Fig. 4B, i) or abrupt (Fig. 4B, ii) increase in brightness (arrows). As Vps8 strongly binds to endosomal membranes, we wondered if some of the Vps8-positive structures at the plasma membrane would correspond to endosomes rather than CORVET alone. We therefore tagged the ESCRT-subunit Vps23 or the Retromer-subunit Vps26 with mCherry (Fig. 4C and D), and observed significant colocalization of endosomal structures at the plasma membrane (see merge pictures). This indicates that Vps8 relocates entire endosomes to the plasma membrane. The latter observation is consistent with individual endosome-endosome fusion or tethering events that are now monitored at the plasma membrane due to the firm association of endosomes and not the vacuole. These data confirm that endosomes tethered via FRB-tagged Vps8 are still functional and provides an opportunity to monitor endosomal biogenesis in a different context. From these findings, we conclude that Vps8 is also tightly associated with endosomal membranes via Vps21, in agreement with previous observations.<sup>35</sup>

### Endogenous HOPS and CORVET are less mobile than individual subunits

We showed before that HOPS subunits like Vps11 and Vps39 were found in the same dot-like structures at the plasma membrane after induced relocalization (Fig. 2F). Due to our experimental setup, which included overexpression of the monitored subunits, we were uncertain if the observed mobility would always reflect the behavior of the entire HOPS or CORVET complex or just single subunits, which nevertheless bind their Rab. We thus tagged the endogenous Vps41 and Vps39 (Fig. 5A and B). Both subunits clearly marked the vacuolar membrane as previously shown.<sup>3</sup> We then addressed their mobility. Addition of 10  $\mu$ M rapamycin resulted in some Vps41 and Vps39 positive dots at the plasma membrane (Fig. 5, white arrows). However, in contrast to our previous observations, where both subunits were relocalized efficiently after 10 min (Fig. 2 and 3), we still observed clear vacuolar staining even after 50 min, indicating that the entire HOPS complex is far less mobile than the individual subunits. Similar results were obtained for Vps11, which is found in CORVET and HOPS,<sup>14</sup> and also for Vps8 (Fig. 5C and D). However, as for the HOPS subunits, a portion of Vps8 (and Vps11) did not become available and remained in endosomal dots throughout the cytoplasm. We thus conclude that both HOPS and CORVET bind preferentially to their target membrane and are far less mobile than previously anticipated.

## Discussion

The dynamics of the vacuolar fusion machinery has been monitored with isolated vacuoles in vitro (e.g.,<sup>36-40</sup>), though the analysis of dynamics in vivo is by far more challenging. Here, we used ligand-induced relocalization to the plasma membrane to monitor the HOPS complex in comparison to the CORVET and Mon1-Ccz1 complexes. Our data reveal that single subunits of both HOPS and CORVET relocalize efficiently to the plasma membrane. For HOPS subunits, this process is enhanced strongly if their respective Rab is lacking or the complex assembly is blocked as in the *vps11 $\Delta$*  mutant (Fig. 3). Among the HOPS subunits, Vps39 seems to be more firmly attached to membranes than Vps41 since Vps39-FRB, but not Vps41-FRB is able to place the vacuole in contact with the plasma membrane and forms patches (Fig. 2). This distinct behavior of Vps39 was also confirmed, when we compared the localization of Ypt7-interacting Vps39 and Vps41 on the vacuole, where we detected Vps39 enriched in distinct spots (Fig. 3). This points to a minimal module for membrane organization at the vacuole, which can be negative for Vps41. The distinct and obviously induced organization patterns of Vps39 and Vps41 may result from dynamic processes of the HOPS and might reflect independent functions of the two proteins apart from their role within the hexameric complex.

Similar to HOPS Vps39, the CORVET subunit Vps8 is tightly associated with endosomes and also triggers the relocalization of the entire organelle to the plasma membrane (Fig. 4). As overexpressed Vps8 strongly clusters endosomes,<sup>35</sup> the kinetics of relocalization might be slowed down. We also tried to follow Vps3 as

the other Rab-specific subunit of CORVET. However, whereas endogenous Vps3 colocalizes completely with Vps8,<sup>32</sup> additional copies accumulated in the cytosol (not shown). We thus did not follow up on the protein's dynamics here.

Interestingly, we observed less dynamics of HOPS and CORVET if we monitored the endogenous subunits. Even though we observed some plasma membrane staining, a large portion of the tethering subunits remained at their target membrane. We consider it unlikely that this is due to the shielding of the respective binding site of the FRB as we observed the same mobility when we swapped the GFP and FRB tag in the tagged protein (not shown). We also noticed that the Mon1-Ccz1 complex, which we used as our initial endosomal probe, was more mobile than HOPS. Relocalization of the complex resulted in a partial shift of Ypt7 from vacuoles to the nuclear ER, indicating that Ypt7 is not activated efficiently. In addition, Mon1-Ccz1 seems to require the endosomal environment or additional interaction partners on endosomes for optimal activity as we did not observe Ypt7 on the plasma membrane after relocalization. This interpretation agrees with the preferential binding of Mon1-Ccz1 to phosphatidylinositol-3-phosphate (PI-3-P) and the stimulated GEF activity on membranes carrying PI-3-P and phosphatidylserine.<sup>41,42</sup> In the previous studies with mitochondrially localized GEFs, the strong activity of the GEF and their overexpression might have favored the efficient Rab recruitment.<sup>11,28</sup>

Our data are consistent with the scenario, in which both HOPS and CORVET mainly exist as a hexameric complex that is bound to vacuoles and endosomes. They are also in agreement with our model (Fig. 2A), in which Vps39 is found proximal to the vacuole membrane, whereas Vps41 is available to bind incoming membranes. Indeed, Vps41 contains a membrane-binding amphipathic lipid packaging sensor (ALPS) motif, which likely supports its interaction with endosomes.<sup>23,43</sup> In addition, Vps41 harbors a conserved interaction site for the AP-3 coat and may bind to incoming AP-3 vesicles.<sup>23,24</sup> HOPS likely uses the available Ypt7-pool to efficiently bind to the vacuole. We showed before that HOPS mobility is increased by phosphorylation via the vacuole-resident Yck3 kinase. In the absence of Yck3, the HOPS subunit Vps41 accumulates at endosome-vacuole contact sites.<sup>39,43</sup> Moreover, without Yck3 or ATP vacuole fusion is highly resistant to Ypt7-inhibitors,<sup>39,43,44</sup> which could be recapitulated partially with proteoliposomes.<sup>18</sup> As a significant pool of endogenous HOPS and overexpressed Vps39 remain on the vacuole surface, we consider it likely that HOPS uses the available Ypt7-GTP pool to remain vacuole-bound during and after fusion. Future studies need to dissect the precise function of the Rab-specific subunits within HOPS (and CORVET) during Rab binding on membranes, tethering and membrane fusion.

## Methods

### Yeast strains and plasmids

*Saccharomyces cerevisiae* strains used in this study are listed in Table 1. All strains were generated using homologs recombination of PCR amplified cassettes<sup>25,45,46</sup> StuI linearized plasmid pRS402 was integrated into the genome of yeast strain HHY110<sup>25</sup> to

**Table 1.** *Saccharomyces cerevisiae* strains

Strain	Genotype	Reference
CUY4655	MATalpha <i>can1-100 leu2-3,112 his3-11,15 ura3 GALpsi<sup>+</sup> tor1-1 fpr1::NAT PMA1-2xFKBP12::TRP1 pRS402::ADE2</i>	This study
CUY4694	MATalpha <i>can1-100 leu2-3,112 his3-11,15 ura3 GALpsi<sup>+</sup> tor1-1 fpr1::NAT PMA1-2xFKBP12::TRP1 pRS402::ADE2 Vps11::FRB-GFP-kanMX</i>	This study
CUY5170	MATalpha <i>can1-100 leu2-3,112 his3-11,15 ura3 GALpsi<sup>+</sup> tor1-1 fpr1::NAT PMA1-2xFKBP12::TRP1 pRS402::ADE2 Vps41::FRB-GFP-kanMX</i>	This study
CUY5178	MATalpha <i>can1-100 leu2-3,112 his3-11,15 GALpsi<sup>+</sup> tor1-1 fpr1::NAT PMA1-2xFKBP12:: TRP1 pRS402::ADE2 VPS11::FRB-GFP-kanMX VPS11::URA3-TEFpr</i>	This study
CUY5199	MATalpha <i>can1-100 leu2-3,112 his3-11,15 ura3 GALpsi<sup>+</sup> tor1-1 fpr1::NAT PMA1-2xFKBP12::TRP1 pRS402::ADE2 VPS8::FRB-GFP-kanMX</i>	This study
CUY5381	MATalpha <i>can1-100 leu2-3,112 his3-11,15 ura3 GALpsi<sup>+</sup> tor1-1 fpr1::NAT PMA1-2xFKBP12::TRP1 pRS402::ADE2 Vps39::FRB-GFP-kanMX</i>	This study
CUY5776	MATalpha <i>can1-100 leu2-3,112 his3-11,15 GALpsi<sup>+</sup> tor1-1 fpr1::NAT PMA1-2xFKBP12:: TRP1 pRS402::ADE2 VPS41::FRB-GFP-kanMX VPS41::URA3-TEFpr</i>	This study
CUY5878	MATalpha <i>can1-100 leu2-3,112 his3-11,15 GALpsi<sup>+</sup> tor1-1 fpr1::NAT PMA1-2xFKBP12:: TRP1 pRS402::ADE2 VPS39::FRB-GFP-kanMX VPS39::URA3-TEFpr</i>	This study
CUY6073	MATalpha <i>can1-100 leu2-3,112 his3-11,15 GALpsi<sup>+</sup> tor1-1 fpr1::NAT PMA1-2xFKBP12::TRP1 pRS402::ADE2 VPS8::FRB-GFP-kanMX VPS8::URA3-TEFpr</i>	This study
CUY6074	MATalpha <i>can1-100 leu2-3,112 his3-11,15 GALpsi<sup>+</sup> tor1-1 fpr1::NAT PMA1-2xFKBP12:: TRP1 pRS402::ADE2 VPS41::FRB-GFP-kanMX VPS41::URA3-TEFpr vps11::hphNT1</i>	This study
CUY6334	MATalpha <i>can1-100 leu2-3,112 GALpsi<sup>+</sup> tor1-1 fpr1::NAT PMA1-2xFKBP12::TRP1 pRS402::ADE2 VPS41::FRB-GFP-kanMX VPS41::URA3-TEFpr ypt7::HIS</i>	This study
CUY6335	MATalpha <i>can1-100 leu2-3,112 GALpsi<sup>+</sup> tor1-1 fpr1::NAT PMA1-2xFKBP12::TRP1 pRS402::ADE2 VPS39::FRB-GFP-kanMX VPS39::URA3-TEFpr ypt7::HIS</i>	This study
CUY6425	MATalpha <i>can1-100 leu2-3,112 his3-11,15 ura3 GALpsi<sup>+</sup> tor1-1 fpr1::NAT PMA1-2xFKBP12::TRP1 pRS402::ADE2 PFK1::FRB-GFP-kanMX</i>	This study
CUY6436	MATalpha <i>can1-100 leu2-3,112 his3-11,15 GALpsi<sup>+</sup> tor1-1 fpr1::NAT PMA1-2xFKBP12:: TRP1 pRS402::ADE2 VPS8::FRB-GFP-kanMX VPS8::URA3-TEFpr vps21::hphNT1</i>	This study
CUY6679	MATalpha <i>can1-100 leu2-3,112 his3-11,15 GALpsi<sup>+</sup> tor1-1 fpr1::NAT PMA1-2xFKBP12::TRP1 pRS402::ADE MON1::FRB-GFP-kanMX MON1::URA3-TEFpr</i>	This study
CUY6876	MATalpha <i>can1-100 leu2-3,112 GALpsi<sup>+</sup> tor1-1 fpr1::NAT PMA1-2xFKBP12::TRP1 pRS402::ADE2 MON1::FRB-kanMX MON1::URA3-TEFpr YPT7::HIS-PHO5pr-GFP</i>	This study
CUY7341	MATalpha <i>can1-100 leu2-3,112 his3-11,15 GALpsi<sup>+</sup> tor1-1 fpr1::NAT PMA1-2xFKBP12:: TRP1 pRS402::ADE2 MON1::FRB-GFP-kanMX MON1::URA3-TEFpr CCZ1::hphNT1-ADHpr-mCherry</i>	This study
CUY7953	MATalpha <i>can1-100 leu2-3,112 his3-11,15 GALpsi<sup>+</sup> tor1-1 fpr1::NAT PMA1-2xFKBP12:: TRP1 pRS402::ADE2 VPS8::FRB-GFP-kanMX VPS8::URA3-TEFpr VAC1::3xmCherry-hphNT1</i>	This study
CUY7721	MATalpha <i>his3Δ200 leu2Δ0 lys2Δ0 met15Δ0 trp1Δ63 ura3Δ0 YPT7pr::TRP1-CET1pr-VC VPS39pr::HIS3-CET1pr-VN</i>	This study
CUY7747	MATalpha <i>his3Δ200 leu2Δ0 lys2Δ0 met15Δ0 trp1Δ63 ura3Δ0 YPT7pr::TRP1-CET1pr-VC VPS39::VN-HIS3MX6</i>	This study
CUY7748	MATalpha <i>his3Δ200 leu2Δ0 lys2Δ0 met15Δ0 trp1Δ63 ura3Δ0 YPT7pr::TRP1-CET1pr-VC VPS41::VN-HIS3MX6</i>	This study
CUY7749	MATalpha <i>his3Δ200 leu2Δ0 lys2Δ0 met15Δ0 trp1Δ63 ura3Δ0 YPT7pr::TRP1-CET1pr-VC VPS39pr::HIS3-CET1pr-VN VPS41::3xmCherry-hphNT1</i>	This study
CUY8632	MATalpha <i>his3Δ200 leu2Δ0 lys2Δ0 met15Δ0 trp1Δ63 ura3Δ0 YPT7pr::TRP1-CET1pr-VC VPS41pr::HIS3-CET1pr-VN</i>	This study
CUY7955	MATalpha <i>can1-100 leu2-3,112 his3-11,15 GALpsi<sup>+</sup> tor1-1 fpr1::NAT PMA1-2xFKBP12:: TRP1 pRS402::ADE2 VPS8::FRB-GFP-kanMX VPS8::URA3-TEFpr VPS23::3xmCherry-hphNT1</i>	This study
CUY7956	MATalpha <i>can1-100 leu2-3,112 his3-11,15 GALpsi<sup>+</sup> tor1-1 fpr1::NAT PMA1-2xFKBP12::TRP1 pRS402::ADE2 VPS8::FRB-GFP-kanMX VPS8::URA3-TEFpr VPS26::3xmCherry-hphNT1</i>	This study
CUY8866	MATalpha <i>can1-100 leu2-3,112 GALpsi<sup>+</sup> tor1-1 fpr1::NAT PMA1-2xFKBP12::TRP1 pRS402::ADE2 MON1::FRB-kanMX MON1::URA3-TEFpr YPT7::HIS-PHO5pr-GFP VPS41::3xmCherry-hphNT1</i>	This study
CUY8898	MATalpha <i>can1-100 leu2-3,112 GALpsi<sup>+</sup> tor1-1 fpr1::NAT PMA1-2xFKBP12::TRP1 pRS402::ADE2 MON1::FRB-kanMX MON1::URA3-TEFpr YPT7::HIS-PHO5pr-GFP SEC63::3xmCherry-hphNT1</i>	This study
CUY9593	MATalpha <i>his3Δ200 leu2Δ0 lys2Δ0 met15Δ0 trp1Δ63 ura3Δ0 YPT7pr::TRP1-CET1pr-VC VPS39::VN-HIS3MX6 VPS39::natNT2-TEFpr</i>	This study
CUY9594	MATalpha <i>his3Δ200 leu2Δ0 lys2Δ0 met15Δ0 trp1Δ63 ura3Δ0 YPT7pr::TRP1-CET1pr-VC VPS41::VN-HIS3MX6 VPS41::natNT2-TEFpr</i>	This study
HHY110	MATalpha <i>ade2-1 can1-100 leu2-3,112 his3-11,15 ura3 GALpsi<sup>+</sup> tor1-1 fpr1::NAT PMA1-2xFKBP12::TRP1</i>	ref. 25

introduce the *ADE2* gene and thus strongly reduce autofluorescence of the vacuole. Split-YFP tags were genomically introduced at the N-terminus of Ypt7, Vps41 and Vps39, or C-terminally added as described.<sup>34</sup>

### Yeast growth and induction of relocalization to the plasma membrane

Yeast strains were grown in YPD over night at 22 °C to early logarithmic phase. The cells were then either spotted directly onto coverslips covered with 0.05% agarose containing YNB medium supplemented with amino acids and indicated rapamycin concentrations, or were resuspended in 0.5 ml YNB (yeast nitrogen base) medium with amino acids and indicated rapamycin concentrations. Staining of yeast vacuoles was performed by addition of 22 µM FM4–64 for 30 min at 22 °C or 0.2 mM CMAC (7-amino-4-Chloromethylcoumarin) for 10 min.

### Microscopy

Cells were imaged on a Leica DM5500 microscope equipped with a 100x objective NA = 1.47, a SPOT Pursuit-XS camera

and filters for GFP, YFP, FM4–64 and mCherry. For acquisition of z-stacks cells were imaged on a DeltaVision Elite microscope equipped with a 60x objective NA = 1.4, a 100x objective NA = 1.49, a sCMOS camera and filters for DAPI, FITC and mCherry. Images were deconvolved using softWoRx software v5.9. From deconvolved z-stacks only one image plain is shown in the figures. Further image processing was performed in ImageJ software (developed by Wayne Rasband, National Institutes of Health, Bethesda, MD, USA).

### Disclosure of Potential Conflicts of Interest

No potential conflicts of interest were disclosed.

### Acknowledgments

We thank Tobias Walther (Yale University, USA) for sharing plasmids. This work was supported by the SFB 944 (project P11), and by the Hans-Mühlenhoff foundation (to CU). JL is supported by the FritzThyssen foundation, Germany.

### References

- Zeigerer A, Gilleron J, Bogorad RL, Marsico G, Nonaka H, Seifert S, Epstein-Barash H, Kuchimanchi S, Peng CG, Ruda VM, et al. Rab5 is necessary for the biogenesis of the endolysosomal system in vivo. *Nature* 2012; 485:465-70; PMID:22622570; <http://dx.doi.org/10.1038/nature11133>
- Huotari J, Helenius A. Endosome maturation. *EMBO J* 2011; 30:3481-500; PMID:21878991; <http://dx.doi.org/10.1038/emboj.2011.286>
- Bröcker C, Kuhlee A, Gatsogiannis C, Balderhaar HJ, Hönscher C, Engelbrecht-Vandré S, Ungermann C, Raunser S. Molecular architecture of the multi-subunit homotypic fusion and vacuole protein sorting (HOPS) tethering complex. *Proc Natl Acad Sci U S A* 2012; 109:1991-6; PMID:22308417; <http://dx.doi.org/10.1073/pnas.1117797109>
- Yu I-M, Hughson FM. Tethering factors as organizers of intracellular vesicular traffic. *Annu Rev Cell Dev Biol* 2010; 26:137-56; PMID:19575650; <http://dx.doi.org/10.1146/annurev.cellbio.042308.113327>
- Barr F, Lambright DG. Rab GEFs and GAPs. *Curr Opin Cell Biol* 2010; 22:461-70; PMID:20466531; <http://dx.doi.org/10.1016/j.ccb.2010.04.007>
- Hutagalung AH, Novick PJ. Role of Rab GTPases in membrane traffic and cell physiology. *Physiol Rev* 2011; 91:119-49; PMID:21248164; <http://dx.doi.org/10.1152/physrev.00059.2009>
- Rink J, Ghigo E, Kalaidzidis Y, Zerial M. Rab conversion as a mechanism of progression from early to late endosomes. *Cell* 2005; 122:735-49; PMID:16143105; <http://dx.doi.org/10.1016/j.cell.2005.06.043>
- Horiuchi H, Lippé R, McBride HM, Rubino M, Woodman P, Stenmark H, Rybin V, Wilm M, Ashman K, Mann M, et al. A novel Rab5 GDP/GTP exchange factor complexed to Rabaptin-5 links nucleotide exchange to effector recruitment and function. *Cell* 1997; 90:1149-59; PMID:9323142; [http://dx.doi.org/10.1016/S0092-8674\(00\)80380-3](http://dx.doi.org/10.1016/S0092-8674(00)80380-3)
- Carney DS, Davies BA, Horazdovsky BF. Vps9 domain-containing proteins: activators of Rab5 GTPases from yeast to neurons. *Trends Cell Biol* 2006; 16:27-35; PMID:16330212; <http://dx.doi.org/10.1016/j.tcb.2005.11.001>
- Nordmann M, Cabrera M, Perz A, Bröcker C, Ostrowicz C, Engelbrecht-Vandré S, Ungermann C. The Mon1-Ccz1 complex is the GEF of the late endosomal Rab7 homolog Ypt7. *Curr Biol* 2010; 20:1654-9; PMID:20797862; <http://dx.doi.org/10.1016/j.cub.2010.08.002>
- Gerondopoulos A, Langemeyer L, Liang J-R, Linford A, Barr FA. BLOC-3 mutated in Hermansky-Pudlak syndrome is a Rab32/38 guanine nucleotide exchange factor. *Curr Biol* 2012; 22:2135-9; PMID:23084991; <http://dx.doi.org/10.1016/j.cub.2012.09.020>
- Wurmser AE, Sato TK, Emr SD. New component of the vacuolar class C-Vps complex couples nucleotide exchange on the Ypt7 GTPase to SNARE-dependent docking and fusion. *J Cell Biol* 2000; 151:551-62; PMID:11062257; <http://dx.doi.org/10.1083/jcb.151.3.551>
- Seals DF, Eitzen G, Margolis N, Wickner WT, Price A. A Ypt/Rab effector complex containing the Sec1 homolog Vps33p is required for homotypic vacuole fusion. *Proc Natl Acad Sci U S A* 2000; 97:9402-7; PMID:10944212; <http://dx.doi.org/10.1073/pnas.97.17.9402>
- Peplowska K, Markgraf DF, Ostrowicz CW, Bange G, Ungermann C. The CORVET tethering complex interacts with the yeast Rab5 homolog Vps21 and is involved in endo-lysosomal biogenesis. *Dev Cell* 2007; 12:739-50; PMID:17488625; <http://dx.doi.org/10.1016/j.devcel.2007.03.006>
- Abenza JF, Galindo A, Pantazopoulou A, Gil C, de los Ríos V, Peñalva MA. Aspergillus RabB Rab5 integrates acquisition of degradative identity with the long distance movement of early endosomes. *Mol Biol Cell* 2010; 21:2756-69; PMID:20534811; <http://dx.doi.org/10.1091/mbc.E10-02-0119>
- Abenza JF, Galindo A, Pinar M, Pantazopoulou A, de los Ríos V, Peñalva MA. Endosomal maturation by Rab conversion in *Aspergillus nidulans* is coupled to dynein-mediated basipetal movement. *Mol Biol Cell* 2012; 23:1889-901; PMID:22456509; <http://dx.doi.org/10.1091/mbc.E11-11-0925>
- Hickey CM, Wickner W. HOPS initiates vacuole docking by tethering membranes before trans-SNARE complex assembly. *Mol Biol Cell* 2010; 21:2297-305; PMID:20462954; <http://dx.doi.org/10.1091/mbc.E10-01-0044>
- Zick M, Wickner W. Phosphorylation of the effector complex HOPS by the vacuolar kinase Yck3p confers Rab nucleotide specificity for vacuole docking and fusion. *Mol Biol Cell* 2012; 23:3429-37; PMID:22787280; <http://dx.doi.org/10.1091/mbc.E12-04-0279>
- Balderhaar HJK, Lachmann J, Yavavli E, Bröcker C, Lürick A, Ungermann C. The CORVET complex promotes tethering and fusion of Rab5/Vps21-positive membranes. *Proc Natl Acad Sci U S A* 2013; 110:3823-8; PMID:23417307; <http://dx.doi.org/10.1073/pnas.1221785110>
- Balderhaar HJK, Ungermann C. CORVET and HOPS tethering complexes - coordinators of endosome and lysosome fusion. *J Cell Sci* 2013; 126:1307-16; PMID:23645161; <http://dx.doi.org/10.1242/jcs.107805>
- Rehling P, Darsow T, Katzmann DJ, Emr SD. Formation of AP-3 transport intermediates requires Vps41 function. *Nat Cell Biol* 1999; 1:346-53; PMID:10559961; <http://dx.doi.org/10.1038/14037>
- Darsow T, Katzmann DJ, Cowles CR, Emr SD. Vps41p function in the alkaline phosphatase pathway requires homo-oligomerization and interaction with AP-3 through two distinct domains. *Mol Biol Cell* 2001; 12:37-51; PMID:11160821; <http://dx.doi.org/10.1091/mbc.12.1.37>
- Cabrera M, Langemeyer L, Mari M, Rethmeier R, Orban I, Perz A, Bröcker C, Griffith J, Klese D, Steinhoff H-J, et al. Phosphorylation of a membrane curvature-sensing motif switches function of the HOPS subunit Vps41 in membrane tethering. *J Cell Biol* 2010; 191:845-59; PMID:21079247; <http://dx.doi.org/10.1083/jcb.201004092>
- Angers CG, Merz AJ. HOPS interacts with Apl5 at the vacuole membrane and is required for consumption of AP-3 transport vesicles. *Mol Biol Cell* 2009; 20:4563-74; PMID:19741093; <http://dx.doi.org/10.1091/mbc.E09-04-0272>
- Haruki H, Nishikawa J, Laemmli UK. The anchor-away technique: rapid, conditional establishment of yeast mutant phenotypes. *Mol Cell* 2008; 31:925-32; PMID:18922474; <http://dx.doi.org/10.1016/j.molcel.2008.07.020>
- Geda P, Patury S, Ma J, Bharucha N, Dobry CJ, Lawson SK, Gestwicki JE, Kumar A. A small molecule-directed approach to control protein localization and function. *Yeast* 2008; 25:577-94; PMID:18668531; <http://dx.doi.org/10.1002/yea.1610>
- Robinson MS, Sahlender DA, Foster SD. Rapid inactivation of proteins by rapamycin-induced rerouting to mitochondria. *Dev Cell* 2010; 18:324-31; PMID:20159602; <http://dx.doi.org/10.1016/j.devcel.2009.12.015>
- Blümer J, Rey J, Dehmelt L, Mazel T, Wu YW, Bastiaens P, Goody RS, Itzen A. RabGEFs are a major determinant for specific Rab membrane targeting. *J Cell Biol* 2013; 200:287-300; PMID:23382462; <http://dx.doi.org/10.1083/jcb.201209113>

29. Ghaemmaghami S, Huh WK, Bower K, Howson RW, Belle A, Dephoure N, O'Shea EK, Weissman JS. Global analysis of protein expression in yeast. *Nature* 2003; 425:737-41; PMID:14562106; <http://dx.doi.org/10.1038/nature02046>
30. Grossmann G, Opekarová M, Malinsky J, Weig-Meckl I, Tanner W. Membrane potential governs lateral segregation of plasma membrane proteins and lipids in yeast. *EMBO J* 2007; 26:1-8; PMID:17170709; <http://dx.doi.org/10.1038/sj.emboj.7601466>
31. Cabrera M, Ungermann C. Guanine nucleotide exchange factors (GEFs) have a critical but not exclusive role in organelle localization of Rab GTPases. *J Biol Chem* 2013; 288:28704-12; PMID:23979137; <http://dx.doi.org/10.1074/jbc.M113.488213>
32. Epp N, Ungermann C. The N-terminal domains of Vps3 and Vps8 are critical for localization and function of the CORVET tethering complex on endosomes. *PLoS One* 2013; 8:e67307; PMID:23840658; <http://dx.doi.org/10.1371/journal.pone.0067307>
33. Ostrowicz CW, Bröcker C, Ahnert F, Nordmann M, Lachmann J, Peplowska K, Perz A, Auffarth K, Engelbrecht-Vandré S, Ungermann C. Defined subunit arrangement and rab interactions are required for functionality of the HOPS tethering complex. *Traffic* 2010; 11:1334-46; PMID:20604902; <http://dx.doi.org/10.1111/j.1600-0854.2010.01097.x>
34. Sung M-K, Huh W-K. Bimolecular fluorescence complementation analysis system for in vivo detection of protein-protein interaction in *Saccharomyces cerevisiae*. *Yeast* 2007; 24:767-75; PMID:17534848; <http://dx.doi.org/10.1002/yea.1504>
35. Markgraf DF, Ahnert F, Arlt H, Mari M, Peplowska K, Epp N, Griffith J, Reggiori F, Ungermann C. The CORVET subunit Vps8 cooperates with the Rab5 homolog Vps21 to induce clustering of late endosomal compartments. *Mol Biol Cell* 2009; 20:5276-89; PMID:19828734; <http://dx.doi.org/10.1091/mbc.E09-06-0521>
36. Price A, Wickner W, Ungermann C. Proteins needed for vesicle budding from the Golgi complex are also required for the docking step of homotypic vacuole fusion. [In Process Citation]. *J Cell Biol* 2000; 148:1223-9; PMID:10725335; <http://dx.doi.org/10.1083/jcb.148.6.1223>
37. Boeddinghaus C, Merz AJ, Laage R, Ungermann C. A cycle of Vam7p release from and PtdIns 3-P-dependent rebinding to the yeast vacuole is required for homotypic vacuole fusion. *J Cell Biol* 2002; 157:79-89; PMID:11916982; <http://dx.doi.org/10.1083/jcb.200112098>
38. Ungermann C, Price A, Wickner W. A new role for a SNARE protein as a regulator of the Ypt7/Rab-dependent stage of docking. *Proc Natl Acad Sci U S A* 2000; 97:8889-91; PMID:10908678; <http://dx.doi.org/10.1073/pnas.160269997>
39. LaGrassa TJ, Ungermann C. The vacuolar kinase Yck3 maintains organelle fragmentation by regulating the HOPS tethering complex. *J Cell Biol* 2005; 168:401-14; PMID:15684030; <http://dx.doi.org/10.1083/jcb.200407141>
40. Thorngren N, Collins KM, Fratti RA, Wickner W, Merz AJ. A soluble SNARE drives rapid docking, bypassing ATP and Sec17/18p for vacuole fusion. *EMBO J* 2004; 23:2765-76; PMID:15241469; <http://dx.doi.org/10.1038/sj.emboj.7600286>
41. Poteryaev D, Datta S, Ackema K, Zerial M, Spang A. Identification of the switch in early-to-late endosome transition. *Cell* 2010; 141:497-508; PMID:20434987; <http://dx.doi.org/10.1016/j.cell.2010.03.011>
42. Cabrera M, Nordmann M, Perz A, Schmedt D, Gerondopoulos A, Barr F, Pichler J, Engelbrecht-Vandré S, Ungermann C. The Mon1-Ccz1 GEF activates the Rab7 GTPase Ypt7 via a longin-fold-Rab interface and association with PI3P-positive membranes. *J Cell Sci* 2014; 127:1043-51; PMID:24413168; <http://dx.doi.org/10.1242/jcs.140921>
43. Cabrera M, Ostrowicz CW, Mari M, LaGrassa TJ, Reggiori F, Ungermann C. Vps41 phosphorylation and the Rab Ypt7 control the targeting of the HOPS complex to endosome-vacuole fusion sites. *Mol Biol Cell* 2009; 20:1937-48; PMID:19193765; <http://dx.doi.org/10.1091/mbc.E08-09-0943>
44. Brett CL, Merz AJ. Osmotic regulation of Rab-mediated organelle docking. *Curr Biol* 2008; 18:1072-7; PMID:18619842; <http://dx.doi.org/10.1016/j.cub.2008.06.050>
45. Janke C, Magiera MM, Rathfelder N, Taxis C, Reber S, Maekawa H, Moreno-Borchart A, Doenges G, Schwob E, Schiebel E, et al. A versatile toolbox for PCR-based tagging of yeast genes: new fluorescent proteins, more markers and promoter substitution cassettes. *Yeast* 2004; 21:947-62; PMID:15334558; <http://dx.doi.org/10.1002/yea.1142>
46. Longtine MS, McKenzie A 3<sup>rd</sup>, Demarini DJ, Shah NG, Wach A, Brachat A, Philippsen P, Pringle JR. Additional modules for versatile and economical PCR-based gene deletion and modification in *Saccharomyces cerevisiae*. *Yeast* 1998; 14:953-61; PMID:9717241; [http://dx.doi.org/10.1002/\(SICI\)1097-0061\(199807\)14:10<953::AID-YEA293>3.0.CO;2-U](http://dx.doi.org/10.1002/(SICI)1097-0061(199807)14:10<953::AID-YEA293>3.0.CO;2-U)